Catalysis Today 423 (2023) 114291

Contents lists available at ScienceDirect

Catalysis Today

journal homepage: www.elsevier.com/locate/cattod

Carbon-supported VPO catalysts with fibrous structure: A new family of catalysts for partial oxidation reactions

M.O. Guerrero-Pérez [a,*], R. Berenguer [b], M.E. Ford [c], I.E. Wachs [c]

[a] Departamento de Ingeniería Química, Universidad de Málaga, E29071, Málaga, Spain
[b] Instituto Universitario de Materiales and Departamento de Química Física, Universidad de Alicante, Apartado 99, E03080 Alicante, Spain
[c] Operando Molecular Spectroscopy & Catalysis Laboratory, Department of Chemical & Biomolecular Engineering, Lehigh University, Bethlehem, PA

ARTICLE INFO

Keywords:
VPO catalysts
Butane oxidation
Carbon materials
Electrospinning

ABSTRACT

The present contribution describes the synthesis of a carbon supported VPO catalyst with a fibrous structure. The synthesis method is simple, low-cost, scalable and reproducible that allows the formation of the bulk mixed oxide $(VO)_2P_2O_7$ (VPP) active phase on the carbon support material. The preparation does not require any special reducing thermal treatments due to the ability of the carbon support to stabilize the VPP active phase since this carbon-based support is stable under oxidizing conditions up to around 400ºC allowing it to be used as for catalytic oxidation reactions. The stability of the carbon-supported VPP catalyst under reaction conditions was examined with *in situ* Raman under oxidizing/ H_2 reducing cycles and n-butane oxidation conditions under both wet and dry conditions. These studies confirm the dynamic character of VPO phases, which interconvert under different conditions, and the stability of carbon-supported VPP phase under different environments. The novel carbon-supported catalyst exhibits an activity behavior like that observed for commercial catalysts that suggests a very promising catalytic material.

1. Introduction

Vanadium oxide-based catalytic materials are well known as active and selective for partial oxidation reactions of alkanes, which are key industrial processes to produce energy and chemical intermediates [1–4]. Oxides of vanadium and phosphorus (VPO) are commercial catalysts for the partial oxidation of n-butane to maleic anhydride [5–8] that finds use for the manufacture of polyester resins, polyurethanes, fibers, and many other products. Several VPO phases have been identified with their properties extensively discussed [6,9] in the literature concluding that bulk vanadyl pyrophosphate, $(VO)_2P_2O_7$ (VPP), is the catalytic active phase [8,9]. In the VPP phase, vanadium is present as V^{4+} and the surface lattice sites are oxidized to V^{5+}. By this manner, a combination of phases in which V adopts V^{5+} and V^{4+} oxidation states improves the catalytic behavior since V can perform redox cycles under reaction conditions; by this way, the surface lattice contributes all of the oxygen to partially oxidize the n-butane, following a Mars van-Krevelen mechanism. An active and selective VPO catalyst usually requires a support in order to mechanically stabilize the VPO mixed oxide phases and to increase the surface area. Additionally, the support may also allow these redox cycles to take place and several supports have been investigated [8]. One attempt was developed by Dupont that synthesized the VPO oxides encapsulated by a porous silica shell [10], which obtained good results in both fixed and fluidized bed reactors. Dupont also developed a technology that consisted of co-feeding pure molecular O_2 in order to keep the catalyst's surface lattice oxidized to maintain a fraction of the pyrophosphate in the V^{5+} oxidation state [11] that gave promising results. However, hot spots in the reactor were found to deactivate the catalysts [12]. Important deactivation issues are that these catalysts undergo phosphorus loss and formation of crystalline V_2O_5 during long term operation. In order to avoid this problem, phosphorus with water is usually added during technical operation [13]. This effect has been attributed to the formation of surface phosphates [14]. Thus, apart from a good activity, selectivity and easily available high surface area, a promising VPO catalytic material needs to satisfy these requirements: i) to be mechanically resistant to physical degradation under reaction conditions, ii) to be produced by a simple and reproducible synthesis method; iii) to show a stabile VPP phase that also allows the VPO phase to oxidize and reduce during reaction conditions, and iv) to remain stable during reaction conditions with and without water. The objective of the present contribution is to describe a carbon-supported VPP catalytic material that addresses these four

* Correspodning author.
E-mail address: oguerrero@uma.es (M.O. Guerrero-Pérez).

https://doi.org/10.1016/j.cattod.2023.114291
Received 16 March 2023; Received in revised form 19 June 2023; Accepted 13 July 2023
Available online 15 July 2023

requirements.

Carbon materials have shown to be promising catalyst supports for several catalytic active phases, including V-containing mixed oxide materials [15]. They are very attractive as catalyst supports since they are inexpensive, have high surface areas, are mechanically stable, and present a rich variety of surface chemical groups that can be easily modified [16]. In addition, if the carbon material contains phosphorous surface groups, easily introduced when it is prepared by chemical activation with phosphorous acid, the carbon oxidation reaction is retarded up to higher temperatures. This enables the utilization of P-containing carbons under oxidizing conditions at moderate reaction temperatures [17]. Particularly, thermogravimetric studies have shown that these materials are stable under oxidizing conditions up to 380 – 390 ºC [17], with phosphorus surface groups preventing carbon from gasification and conferring a high oxidation resistance [18].

By this manner, vanadium oxides supported on phosphorous containing carbon materials have been demonstrated as promising catalytic materials [17]. With the aim of overcoming the limitations of the supported VPO catalytic materials that have been commercially available up to date, this work poses the design of a catalytic material that is inexpensive and stable under reaction conditions, and that additionally allows the V^{4+}-V^{5+} redox cycle required for catalyzing n-butane to maleic anhydride.

To investigate this novel approach, the main objective of the present work is the study of the preparation, properties and performance (activity, selectivity and stability) of new carbon-supported VPO catalysts with fibrous structure. Particularly, special effort is devoted to demonstrate the reversibility and stability of VPO phases, in the proposed material, for the catalytic conversion of n-butane. The fibrous carbon support can be prepared quite easily by electrospinning technique [19], which is quite versatile and easy to handle [20], and by using lignin as a renewable and low-cost carbon precursor. The fibrous morphology provides low resistance for internal diffusion and high surface area and accessibility of VPO phases. Furthermore, the effective introduction of surface P functionalities on the carbon support greatly increases its thermal stability under different conditions.

2. Experimental

2.1. Synthesis of materials

The carbon supported VPO material was prepared following a procedure optimized in a previous study [20]. In a first stage, a P containing carbon fiber material was prepared by electrospinning of a solution of lignin/H_3PO_4 (1/0.3 wt%) in ethanol, followed by a heat treatment (200ºC for 1 h in air and then up to 900ºC at 10º/min heating ramp in N_2 for carbonization) in a horizontal furnace with a flow of the corresponding gas treatment of 150 cc (STP)/min. Lignin was chosen as carbon source since it is a waste obtained during paper manufacture. Then, the obtained P-carbon fibrous material (PCF) was washed with hot distilled water to remove all the non-anchored species and dried in static-air (80ºC) overnight. In a second step, this phosphorous containing carbon was impregnated (in a rotatory evaporator (at 80ºC and 30 mm Hg) with a solution of NH_4VO_3 (99.99%, Sigma- Aldrich) in 0.5 M oxalic acid (99% Sigma Aldrich). Considering the surface area of the carbon fibers, 1100 m^2/g, the amount of vanadium to impregnate was calculated in order to obtain a material with 4 V atoms per nm^2 of support, since a previous study [15] concluded that this is the maximum amount of vanadium oxide species that remain dispersed avoiding the formation of V_2O_5 crystals. Then, the V impregnated carbon fibers (V/PCF) were treated in flowing-air (150 cc (STP)/min) at 200ºC for 2 h. This material, referred to as V/PCF, has a BET surface area of 790 m^2/g.

In order to study the effect of the carbon support, a bulk oxide VPO material was prepared by calcination in air for 1 h (heating ramp 3ºC/min) at 500ºC of V/PCF material. This calcination methodology was optimized in a previous study [20] in order to eliminate the carbon material but maintaining the fibrous morphology of the material. This VPO material has a BET surface area of 62 m^2/g.

2.2. Characterization

Activity measurements were performed in a quartz microreactor with 9 mm of diameter with 300 mg of catalyst (particle dimensions in the 0.25–0.125 mm range) with on-line gas chromatograph equipped with two different columns. Hydrocarbons and oxygenates were analyzed with a FID detector whereas CO, CO_2, H_2O and O_2 were analyzed with a TCD detector. Activity was measured after 30 min of time on stream at 380ºC. Each analysis took 40 min. The activity was measured during time on stream for six hours and the results remained stable within the error of determinations (± 10%). The axial temperature profile was monitored by a thermocouple sliding inside a tube inserted into the catalytic bed. The feed composition was 2% of n-butane, 15% of oxygen, and balanced in He. A total flow of 30 mL/min of reactants fed through gas flow controllers was used. The quantity of catalyst and total flow were determined in order to avoid internal and external diffusion contributions. Butane conversion and selectivity values were determined based on the moles of n-butane feed and products, considering the number of carbon atoms in each molecule. The correctness of the analytical determinations was checked for each test by verification that the carbon balance (based on the propane converted) was within the cumulative mean error of the determinations (± 10%).

N_2 adsoption/desorption isotherms for PCF and V/PCF calcined materials were obtained at − 196ºC in an ASAP 2020 Micromeritics Instrument. The samples were previously outgassed at 150ºC for 8 h. The morphology was studied by scanning electron microscopy (SEM) and by transmission electron microscopy (TEM). SEM images were obtained using a JEOL JSM-840 instrument, working at a high voltage of 20–25 kV whereas TEM analyses were carried out in a CM200 apparatus (Philips). X-ray photoelectron spectroscopy (XPS) analyses of the calcined samples were obtained using a 5700 C model Physical Electronics apparatus, with MgKα radiation (1253.6 eV). For the analysis of the XPS peaks, the C1s peak position was set at 284.5 eV and used as reference to position the other peaks while the fitting of the XPS peaks was done by least squares using Gaussian-Lorentzian peak shapes.

In situ Raman spectra (532 nm laser excitation) were obtained with a high-resolution, dispersive Raman spectrometer system (HoribaJovin Yvon LabRam HR) equipped with a confocal microscope (Olympus BX-30), notch filter (Kaiser SuperNotch) and a 900 groves/mm grating. The laser excitation was generated with a Nd-YAG double diode pumped laser (Coherent Compass 315 M-150, output power of 150 mW, with sample power 10 mW). The scattered photons were directed onto a single monochrometer and focused onto a UV-sensitive liquid N_2 cooled detector (HoribaJovin Yvon CCD3000-V) with a spectral resolution of ~2 cm^{-1} for the given parameters. The notch filter has a ~100 cm^{-1} cutoff for visible spectra; Raman spectra were collected above 200 cm^{-1}. The catalysts were evaluated as loose powders in an environmental chamber (Harrick HVC-DR2, with a CaF_2 window) under the conditions shown below. The temperature of the environmental cell was controlled with a Harrick ATC temperature controller. Spectral collection times were typically 30 s per scan with five scans.

2.3. Experimental procedure for catalyst reduction and reoxidation

After heating (10 C/min) to 300 C under flowing 10% O_2/Ar (30 mL/min) for 1 hr, the sample was cooled to 110 C, the 10% O_2/Ar replaced with flowing Ar (30 mL/min) and flushed with flowing Ar for 15 min. Subsequently, Ar was replaced with flowing 10% H_2/Ar (30 mL/min), the sample heated to 125 C, held at 125 C for 10 min and a Raman spectrum recorded. The sample was then heated stepwise in 25 C intervals to either 175 C or 200 C and was held at each of these steps for 10 min before a Raman spectrum was recorded. At the end of this sequence, the sample was cooled to 110 C under flowing 10% H_2/Ar, the H_2/Ar

replaced with flowing Ar (30 mL/min) and the sample was flushed with flowing Ar for 15 min. Reoxidation was carried out by replacing the Ar flow with flowing 10% O_2/Ar (30 mL/min). The sample was heated to 125 C, held at 125 C for 10 min, and a Raman spectrum was recorded. The sample was then heated stepwise in 25 C intervals to either 175 C or 200 C and was held at each of these steps for 10 min before a Raman spectrum was recorded. Finally, the sample was cooled to 110 C. If desired, a second reduction step was carried out using the conditions described immediately above.

2.4. Experimental procedure for the dehydration/oxidation cycles and oxidation of n-butane

Dehydration (procedure 1, P1). The sample was heated to 100 C, 200 C, and then 300 C (10ºC/min) under flowing (30 mL/min) 10% O_2/Ar. Raman spectra (532 nm laser) were taken at each of those temperatures. The sample was maintained at 100 C and 200 C just long enough to record the spectrum; and heating was resumed immediately after the spectrum had been obtained. Upon reaching 300 C, the sample was held at 300 C for an hour under flowing (30 mL/min) 10% O_2/Ar. In addition to the Raman spectrum taken when the sample reached 300 C, spectra were taken after 30 min and 60 min. After cooling to 110 C, a Raman spectrum was taken of the dehydrated catalyst while it was still under flowing 10%O_2/Ar. As expected, the peaks were sharper and the resolution better at 110 C. Next, the sample was flushed with flowing Ar (30 mL/min) for 15 min

Oxidation of n-butane under wet conditions (procedure 2, P2). Upon completion of the dehydration procedure, the feed to the cell was switched to a mixture of 10% n-butane/nitrogen (10 mL/min) and air (31 mL/min), for a total flow of 41 mL/min (15% O_2 in feed). By this way the composition in terms of butane/oxygen ratio is similar to that used in the fixed bed experiments. The mixed feed was passed through a bubbler which contained deionized water, and which was maintained at 43 C with a heated water bath. The vapor pressure of water at 43ºC was 64.8 mm, which gave 8.5% water in the feed. After switching to this feed composition, the catalyst was heated to 300 C (10 C/min). Immediately upon reaching 300 C, a Raman spectrum was taken. Subsequently, Raman spectra were recorded at intervals over 90 min. Upon completion of this procedure, oxidation under dry conditions was begun. Oxidation of n-butane under dry conditions (procedure 3, P3). The catalyst was maintained under the conditions of P2, with the exception that the bubbler was bypassed, and dry feed was introduced into the cell. Spectra were recorded at intervals over the next 2 hrs. As the dry reaction progresses, note the reappearance of VPO features, starting with the peak at 930 cm^{-1}. At the end of this time, the feed to the cell was switched to Ar (30 mL/min), and the cell was flushed with Ar for 15 min

Final dehydration (procedure 4, P4). After flushing with Ar for 15 min, the feed was switched to 10% O_2/Ar (30 mL/min). Raman spectra were then recorded at 300 C (1 min, 30 min) and after cooling to 110 C.

3. Results and Discussion

3.1. Characterization of catalysts

The BET surface areas, XPS composition of the surface regions, and catalytic activity performance are presented in Table 1 for both V/PCF and VPO materials. The formation of vanadium-phosphorus mixed oxide (VPO) species in these materials was confirmed by XPS (supporting information (SI)). As expected, the surface area of the unsupported, bulk material VPO phase is much lower than that for the supported V/PCF catalyst. The activity results for the bulk VPO sample are like those reported for similar samples [21]. Table 1 data shows that at the same reaction temperature, supported V/PCF performs much better in terms of n-butane activity and maleic anhydride selectivity, showing catalytic results comparable to those obtained with commercial VPO catalysts after activation [11,13]. Thermogravimetric studies with similar samples have shown that these carbon supported materials are stable under oxidizing conditions up to 380 – 390 ºC [20] since phosphorus surface groups prevent carbon gasification and thus confer a high oxidation resistance to these phosphorous carbon materials [21,22]. XPS results confirm that P is incorporated to the carbon surface during the chemical activation step with phosphoric acid. Previous studies have revealed that it forms different surface functionalities like -C-O-P, C-P-O and C_3PO [21,22] (Fig. 1 SI).

Fig. 1 A and 1B show SEM images of the V/PCF material, confirming the fibrous morphology with diameters in the 300 nm – 3 μm range. As can be observed in the images, the vanadium impregnation after the carbon fiber synthesis does not alter the fibrous morphology. The images (Fig. 1B) also demonstrate how the vanadium oxide is distributed quite uniformly over the surface of the carbon fibers. TEM (Fig. 1C) confirms that the sample is composed by a carbon fiber covered by a film that forms some clusters/aggregated, whose SAED (Fig. 1D) reveals a diffuse ring pattern, that could be associated with an amorphous or nanocrystalline material.

3.2. In situ Raman: dehydration/oxidation cycles

The supported V/PCF catalyst was examined with *in situ* Raman during dehydration/oxidation cycles following the procedure described in the experimental section (P1-P3). The dehydrated spectrum (Fig. 2A) shows the presence of the carbon support (broad Raman bands near 1330 and 1590 cm^{-1}) and a band near 934 cm^{-1} from the crystalline $(VO)_2P_2O_7$ (VPP) phase [12]. When the temperature is increased under reducing conditions (Fig. 2A), the Raman band of $(VO)_2P_2O_7$ becomes more intense, especially around 150ºC, as expected, since V species remain reduced as V^{4+} in $(VO)_2P_2O_7$ mixed phase. Some signals near 995 and 1090 cm^{-1} can be also observed at 125 and 150ºC that are from the crystalline αII-$VOPO_4$ phase. This is indicative of the dynamic character of VPO phases. It is well known that an active and selective VPO catalyst requires that these mixed oxide phases interconvert under different reaction conditions of temperature, atmosphere and pressure. The dynamic character of VPO phases in the novel V/PCF material is also illustrated in Fig. 2B since under a re-oxidation cycle and subsequent reduction, the bands of the crystalline $(VO)_2P_2O_7$ and $\alpha_{II}VOPO_4$ phases are not visible under the oxidation cycle and only become visible under reducing conditions. (Table 2).

The dehydration/oxidation *in situ* Raman study was also performed with bulk sample VPO in order to analyze the effect of carbon support and Fig. 3 shows the results. Fig. 3A shows the dehydrated sample (black spectrum), dominated by a sharp band near 980 cm^{-1}, that is attributed to $VO(HPO_4)\bullet 0.5\ H_2O$ phase [23]. This phase is stable under reducing conditions up to 150ºC (Fig. 3A) and at 200ºC the shape of the spectrum is quite different. The Raman band near 934 cm^{-1} belongs mainly to the crystalline $(VO)_2P_2O_7$ phase. In addition, bands near 1131, 1039 and

Table 1
BET surface area values calculated from the N_2 isotherms, atomic elemental compositions (%) of the surface region determined by XPS, of calcined samples, and catalytic performance (n-butane conversion and selectivity to maleic anhydride, CO and CO_2) after 30 min of time on stream at 380ºC.

	BET A (m^2/g)	C (1 s)	O (1 s)	N (1 s)	V[2p]	P[2p]	CBu (%)	C_{CO}	C_{CO2}	SMA (%)
V/PCF	790	79	16	1	2	2	79	18	10	72
VPO	62	21	56	3	7	13	41	23	12	65

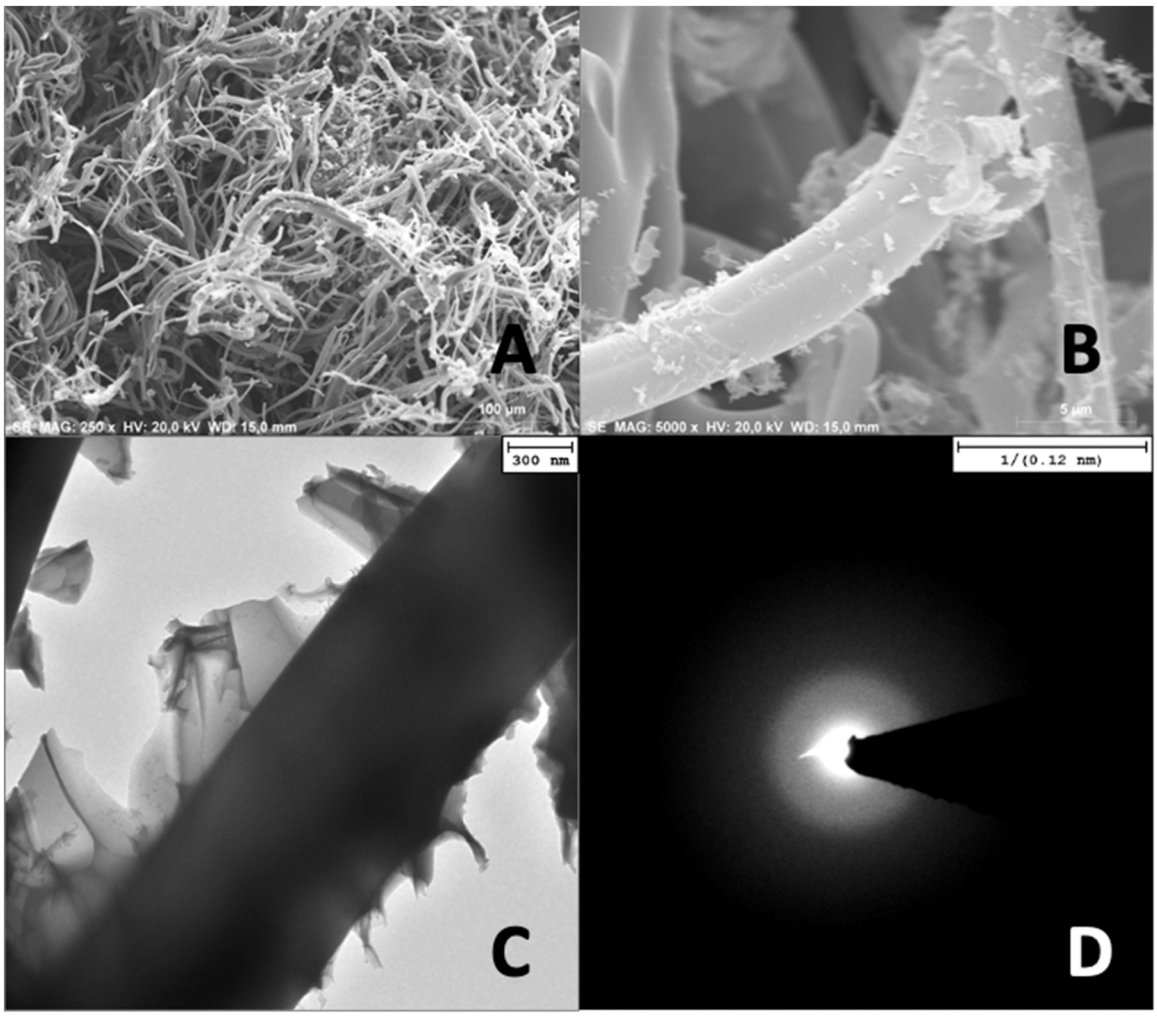

Fig. 1. SEM low-magnified (A) and magnified (B) and TEM (C-D) images of V/PCF material.

980 cm^{-1} are also visible and these bands may indicate a mixture of VPO phases in which vanadium is present as V^{5+} (*e.g.*, $\alpha_{II}VOPO_4$ (Raman bands near 990 and 1100 cm^{-1}), β $VOPO_4$ (Raman bands near 990 and 1070 cm^{-1}), γ $VOPO_4$ (Raman bands near 938, 1032 and 1085 cm^{-1}) and δ $VOPO_4$ (935, 1020 and 1085 cm^{-1}) [20]. The bands in the 600 – 100 cm^{-1} range are also attributed to a mixture of these phases [12,13, 23]. Fig. 3B shows the spectra during re-oxidation and, as can be observed, the Raman band at 980 cm^{-1} is restored. During a second reduction treatment (Fig. 3C), this band again disappears giving rise to the bands assigned to a mixture of several VPO phases. The Raman spectra confirm the dynamic character of VPO phases in VPO materials. The main difference with respect V/PCF sample (Fig. 2) is that in the case of bulk material (Fig. 3), spectra are not dominated by the Raman band due to $(VO)_2P_2O_7$. This may indicate that carbon support is able to stabilize this VPP phase.

3.3. *In situ* Raman under Butane Oxidation reaction

In situ Raman spectra were recorded in order to further investigate the stability of the supported V/PCF catalysts under n-butane oxidation reaction conditions. Fig. 4A shows the dehydration treatment *versus* time on stream of V/PCF sample at 300ºC. In agreement with the results obtained at lower temperatures, it can be observed how during the thermal treatment, the VPP band (931 cm^{-1}) increases whereas the band near 992 cm^{-1}, assigned to VPO phases in which Vanadium species are as V^{5+}, tend to disappear. Under reaction conditions (Fig. 4B), it can be observed how the formation of VPP phase also occurs and in a higher extent. After two hours under reaction conditions, other small features are detected in the spectrum that could be indicative that, at a minor extent, other VOx (Vanadium oxide dispersed species) and/or VPO phases may form. After reaction, the catalyst was re-oxidized (Fig. 4C) to further investigate its dynamic structure. Fig. 4C shows that the spectrum of the catalysts after reaction is similar to that obtained before (Fig. 4A), with the Raman bands due to the carbon support (1600 and 1330 cm^{-1}) and to crystalline $(VO)_2P_2O_7$ (band near 930 cm^{-1}). These data clearly demonstrate that the supported V/PCF catalyst is stable under n-butane oxidation reaction.

To prevent VPO catalyst deactivation by loss of phosphorous and subsequent V_2O_5 formation, addition of water in the reactants feed has been proposed with the aim of keeping phosphorus distributed on the surface of the catalysts [14,24,25]. However, this can affect the distribution of VPO mixed phases and subsequently the selectivity of the catalyst. To further investigate the addition of water under reaction conditions on the structure of V/PCF sample, an *in situ* Raman study was also performed under wet butane oxidation reaction according to the procedure described as P2 in the experimental section. During the first 30 min under wet butane oxidation conditions (Fig. 5A) the Raman bands near 1609 and 1552 cm^{-1} due to carbon support, and the band near 930 cm^{-1} that belongs to VPP active phase dominate the spectrum, although other bands assigned to several VPO phases are also visible. To further analyze the effect of water on the distribution of VPO species, Fig. 5B compares the spectrum taken under dehydration conditions at

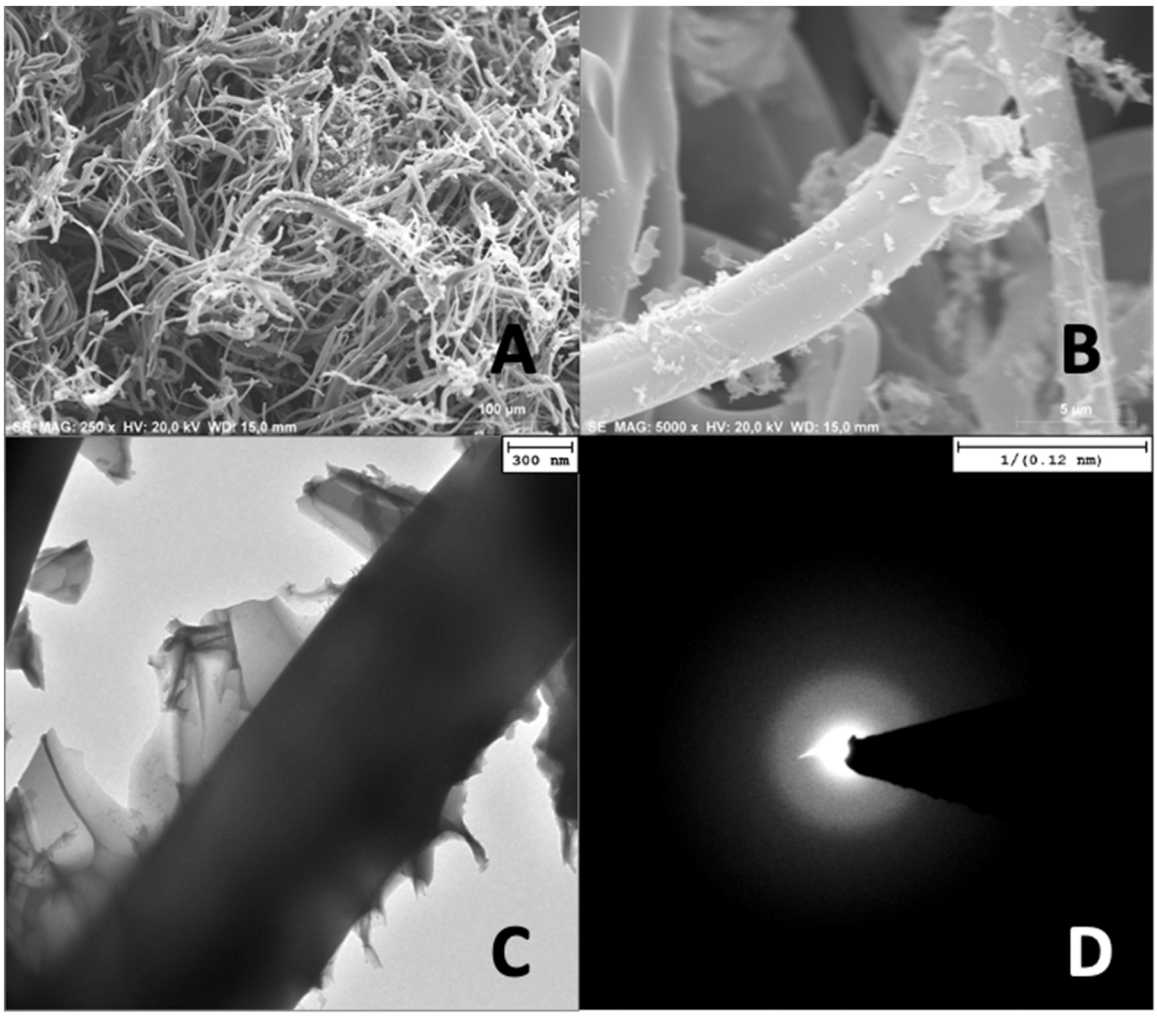

Fig. 2. Raman spectra of V/PCF sample under different conditions. (A) Dehydration and first reduction and (B) re-oxidation and second reduction.

Table 2
Raman bands assigned to VPO phases (according to Ref. 23).

Reference VPO phase	Raman bands (cm^{-1})
$(VO)_2P_2O_7$ (VPP)	934
αII-$VOPO_4$ phase	995, 1090
β $VOPO_4$	990, 1070
γ $VOPO_4$	938, 1032, 1085
δ $VOPO_4$	935, 1020, 1085
$VO(HPO_4)$•0.5 H_2O phase	980

110ºC with the spectrum obtained under wet butane oxidation conditions at 300ºC at the start of the reaction. These show that during the first minute under wet conditions, Raman bands near 1059, 987, 643, 421, 353, 313 and 281 cm^{-1} appear, in addition to the Raman band near 930 cm^{-1} due to VPP phase. As has been already discussed, these bands may indicate a mixture of VPO phases in which vanadium is present as V^{5+}, such as $\alpha_{II}VOPO_4$ (Raman bands near 990 and 1100 cm^{-1}), β $VOPO_4$ (Raman bands near 990 and 1070 cm^{-1}), γ $VOPO_4$ (Raman bands near 938, 1032 and 1085 cm^{-1}) and δ $VOPO_4$ (935, 1020 and 1085 cm^{-1}) [20]. This could indicate that under wet conditions, vanadium species tend to partially oxidize, and, it should be noted that for V/PCF sample, these VPO species with V^{5+} were not detected under dry oxidation conditions (Fig. 4). Fig. 5C shows that, after reaction under wet conditions and subsequent reoxidation, a spectrum similar to that of the dehydrated fresh sample (Fig. 5B) is obtained. This spectrum is dominated by the Raman bands of the carbon support and VPP phase, thus demonstrating that the formation of other VPO phases in addition to VPP in which V species are oxidized under wet conditions, is temporal and reversible.

4. Conclusions

This work describes the fabrication methodology and outstanding catalytic properties of new carbon-supported VPO catalysts with fibrous structure. The methodology is based on the preparation of P-doped carbon fibers, by electrospinning of lignin/H_3PO_4 solutions, followed by the effective dispersion of VPO phases. Exhaustive Raman characterization shows that the fibrous carbon support obtained by this method is efficient to stabilize a highly dynamic $(VO)_2P_2O_7$ (VPP) active phase under several reaction conditions (both dry and wet) and oxidation/reduction cycles. The presence of this stabilized active phase can be associated to the higher n-butane conversion activity and selectivity towards maleic anhydride found for the proposed fibrous catalyst, as compared to a similar catalyst without carbon. Such extraordinary stabilizing effects are assigned not only to the carbon support itself, but also to the presence of uniformly distributed surface phosphorus groups, introduced by the proposed method, that confer this support with a high oxidation resistance.

The obtained results highlight the benefits of using carbon materials as supports of VPO catalysts. Particularly, unlike most synthesis methods of VPP phases, the carbon-supported VPO catalyst proposed in this work can be easily prepared without using reductant conditions and/or

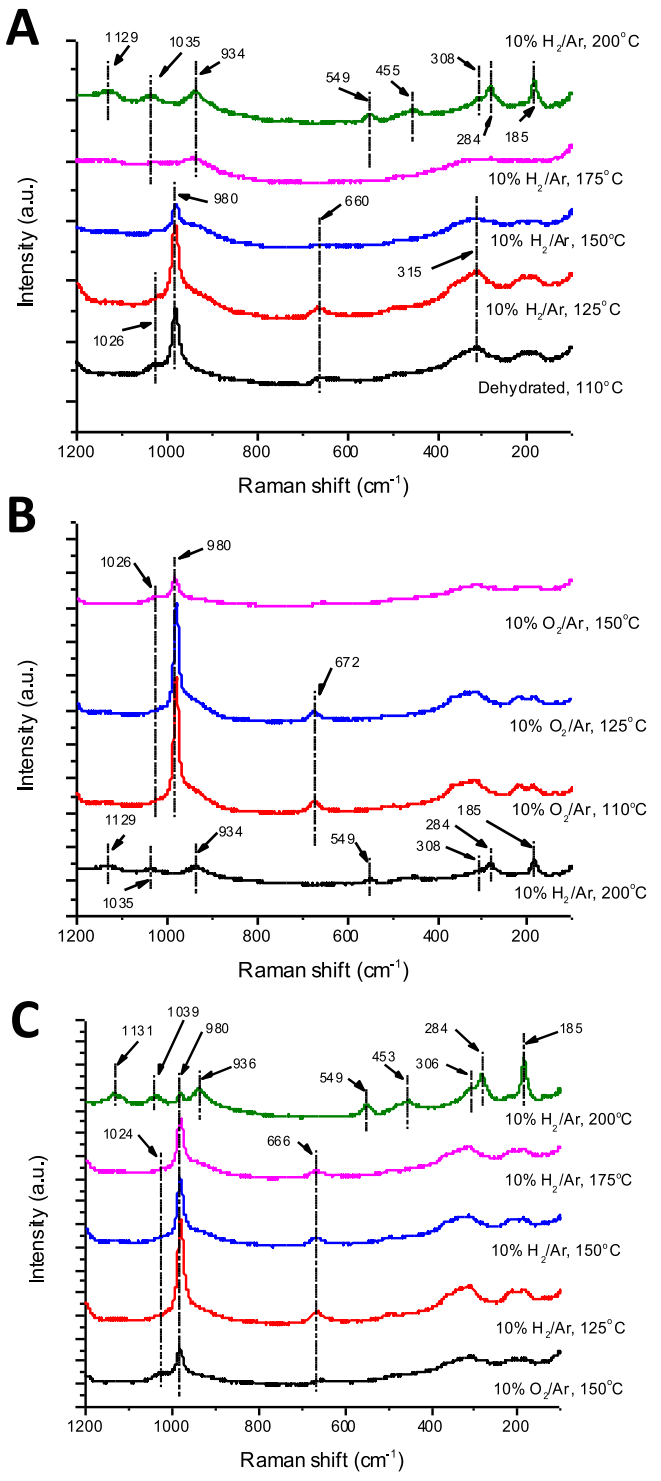

Fig. 3. Raman spectra of bulk VPO sample under different conditions. (A) Dehydration and first reduction and (B) re-oxidation and (C) second reduction.

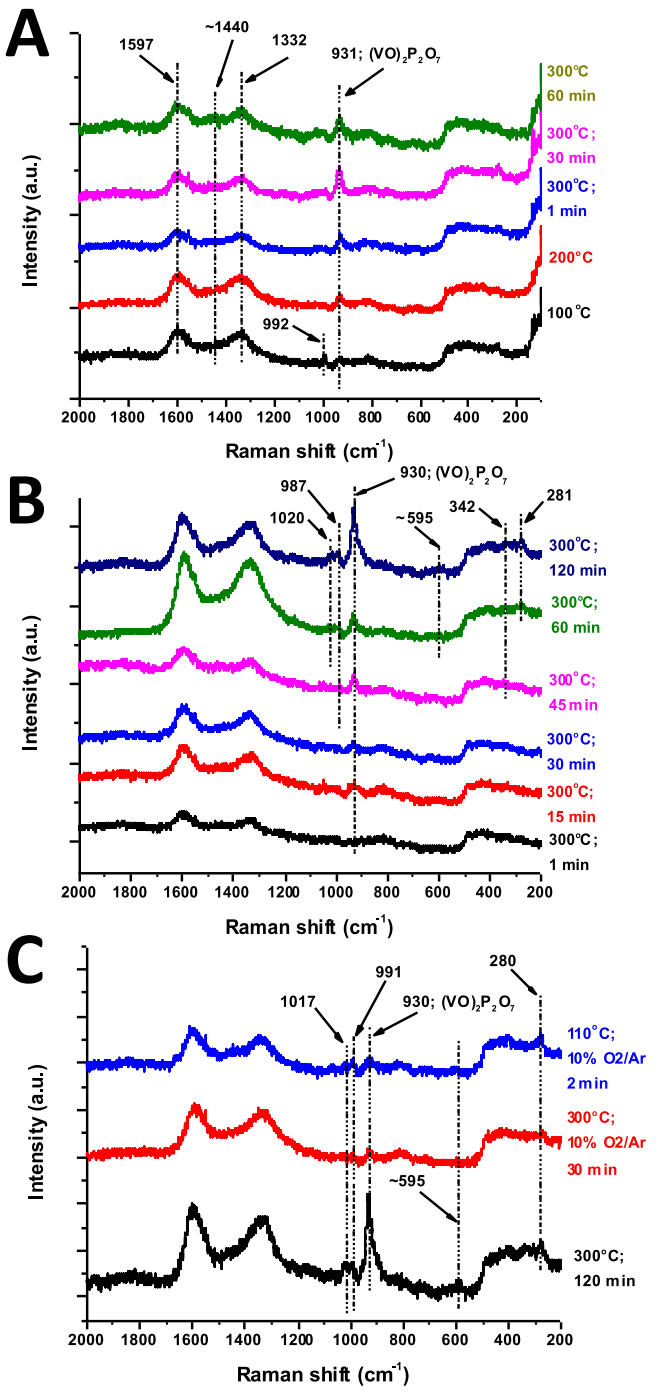

Fig. 4. Raman spectra of V/PCF sample (A) under dehydration at 300ºC (procedure P1) (B) dry butane oxidation (procedure P3) (C) dehydration after dry oxidation reaction at 300 ºC.

activation for long periods. In addition, it exhibits an excellent mechanical stability. The used electrospinning method can be easily handled and scaled up at industrial scale, and the fibrous morphology involves several benefits in terms of catalyst surface area and accessibility, and internal gas diffusion. Furthermore, the utilization of lignin as carbon precursor is advantageous from the economic and environmental points of view.

CRediT authorship contribution statement

All authors have participated in the analysis and interpretation of the experimental data and have revised the final version of the manuscript. MEF and IEW have performed the Raman study, RB and MOGP have participated in the synthesis and characterization of the catalysts.

Declaration of Competing Interest

The authors declare the following financial interests/personal relationships which may be considered as potential competing interests:

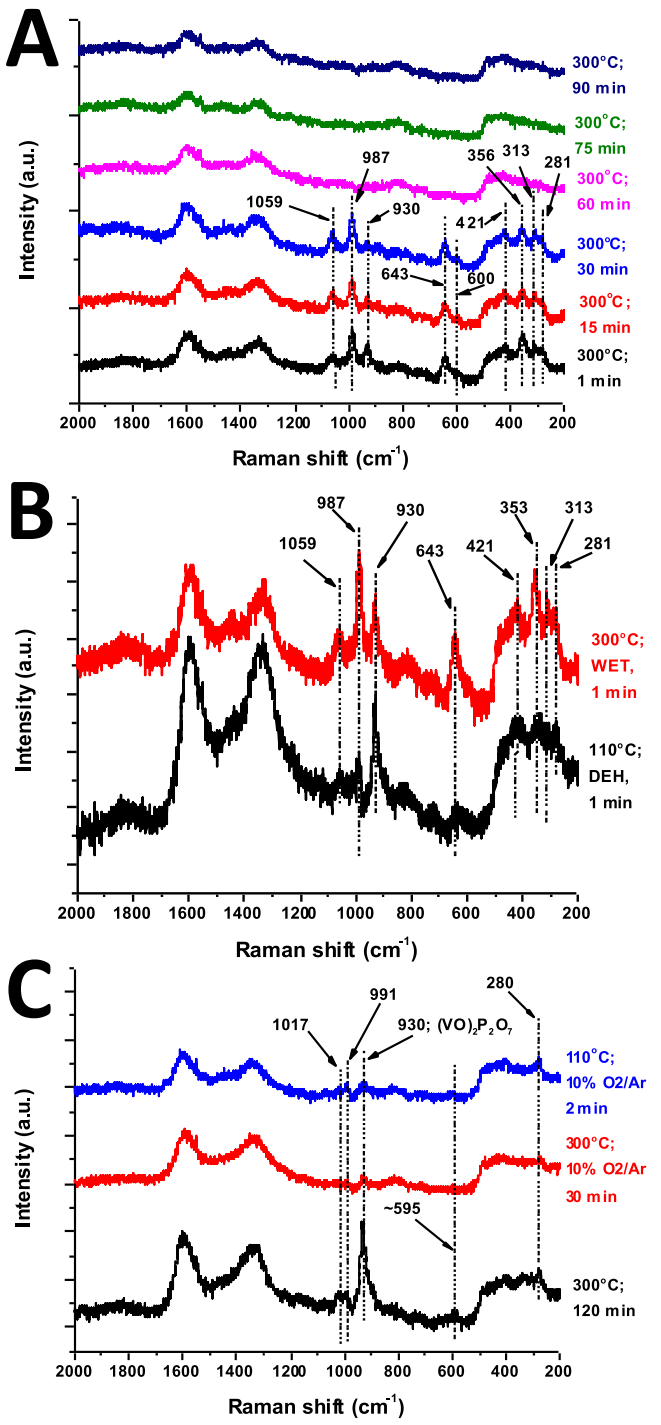

Fig. 5. Raman spectra of V/PCF sample (A) under *in situ* n-butane wet oxidation at 300ºC (procedure P2) (B) comparison of spectra taken under dehydration conditions at 110ºC and wet n-butane oxidation conditions at 300ºC at the start of reaction, and (C) dehydration after wet oxidation reaction at 300ºC.

M. Olga Guerrero Perez reports financial support was provided by Government of Andalusia and Spanish Ministry of Science. Raul Berenguer reports financial support was provided by Spain Ministry of Science and Innovation and Generalitat Valenciana.

Data Availability

No data was used for the research described in the article.

Acknowledgements

MOGP to TED2021–130756B-C31 (MCIN/AEI/10.13039/501100011033) and PID2020–118593RB-C22 (MCIN/AEI/10.13039/501100011033); and P20_00375 (Junta de Andalucía, Spain). RBB to EDGJID/2021/330 (Generalitat Valenciana, Spain), as well as the RYC-2017–23618 contract and TED2021–131028B-I00 project funded by MCIN/AEI/10.13039/501100011033 and "ESF Investing in your future" and "European Union NextGeneration EU/PRTR".

Dedication

This article is dedicated to Prof. David Tudela Moreno, from the Universidad Autónoma de Madrid, who has been for many years a source of scientific inspiration for many of the students, as MOGP, that were lucky enough to have him as professor of Inorganic Chemistry.

Appendix A. Supporting information

Supplementary data associated with this article can be found in the online version at doi:10.1016/j.cattod.2023.114291.

References

[1] A. Chakrabarti, M.E. Ford, D. Gregory, R. Hu, C.J. Keturakis, S. Lwin, Y. Tang, Z. Yang, M. Zhu, M.A. Bañares, I.E. Wachs, A decade+ of operando spectroscopy studies, Catal. Today 283 (2017) 27–53, https://doi.org/10.1016/j.cattod.2016.12.012.
[2] M.O. Guerrero-Pérez, Supported, bulk and bulk-supported vanadium oxide catalysts: a short review with an historical perspective, Catal. Today 285 (2017) 226–233, https://doi.org/10.1016/j.cattod.2017.01.037.
[3] C.A. Carrero, R. Schloegl, I.E. Wachs, R. Schomaecker, Critical literature review of the kinetics for the oxidative dehydrogenation of propane over well-defined supported vanadium oxide catalysts, ACS Catal. 4 (2014) 3357–3380, https://doi.org/10.1021/cs5003417.
[4] I.E. Wachs, Y. Chen, J.M. Jehng, L.E. Briand, T. Tanaka, Molecular structure and reactivity of the Group V metal oxides, Catal. Today 78 (2003) 13–24, https://doi.org/10.1016/S0920-5861(02)00337-1.
[5] W.H. Cheng, Effect of compositions of promoted VPO catalysts on the selective oxidation of n-butane to maleic anhydride, Appl. Catal. A: Gen. 147 (1996) 55–67, https://doi.org/10.1016/S0926-860X(96)00213-X.
[6] V.V. Guliants, J.B. Benziger, S. Sundaresan, I.E. Wachs, J.M. Jehng, J.E. Roberts, The effect of the phase composition of model VPO catalysts for partial oxidation of n-butane, Catal. Today 28 (1996) 275–295, https://doi.org/10.1016/S0920-5861(96)00043-0.
[7] J.B. Benziger, V. Guliants, S. Sundaresan, New precursors to vanadium phosphorus oxide catalysts, Catal. Today 33 (1997) 49–56, https://doi.org/10.1016/S0920-5861(96)00135-6.
[8] G. Centi, Vanadyl pyrophosphate - a critical overview, Catal. Today 16 (1993) 5–26, https://doi.org/10.1016/0920-5861(93)85002-H.
[9] G. Centi, Some prospects and priorities for future research on vanadyl pyrophosphate, Catal. Today 16 (1993) 147–153, https://doi.org/10.1016/0920-5861(93)85015-R.
[10] N.F. Dummer, W. Weng, C. Kiely, A.F. Carley, J.K. Bartley, C.J. Kiely, G. J. Hutchings, Structural evolution and catalytic performance. Of DuPont V-P-O/SiO2 materials designed for fluidized bed applications, Appl. Catal. A: Gen. 376 (2010) 47–55, https://doi.org/10.1016/j.apcata.2009.10.004.
[11] G.S. Patience, R.E. Bockrath, "Butane oxidation process development in a circulating fluidized bed, Appl. Catal. A: Gen. 376 (2010) 4–12, https://doi.org/10.1016/j.apcata.2009.10.023.
[12] S. Badehbakhsh, N. Saadatkhah, M.J.D. Mahboub, O. Guerrero-Pérez, G. S. Patience, Morphological changes of vanadyl pyrophosphate due to thermal excursions, Catal. Today 407 (2023) 301–311, https://doi.org/10.1016/j.cattod.2021.12.008.
[13] D. Lesser, G. Mestl, T. Turek, Transient behaviour of vanadyl pyrophosphate catalysts during the partial oxidation of n-butane in industrial-sized, fixed bed reactors, Appl. Catal. A 510 (2016) 1–10, https://doi.org/10.1016/j.apcata.2015.11.002.
[14] F. Cavani, S. Luciani, E.D. Esposti, C. Cortelli, R. Leanza, Surface dynamics of a vanadyl pyrophosphate catalyst for n-butane oxidation to maleic anhydride: an in situ raman and reactivity study of the effect of the P/V atomic ratio, Chem. A Eur. J. 16 (2010) 1646–1655, https://doi.org/10.1002/chem.200902017.
[15] M.O. Guerrero-Pérez, J.M. Rosas, R. López-Medina, M.A. Bañares, J. Rodríguez-Mirasol, T. Cordero, On the nature of surface vanadium oxide species on carbons, J. Phys. Chem. C. 116 (2012) 20396–20403, https://doi.org/10.1021/jp305853b.
[16] F. Rodriguez-Reinoso, The role of carbon materials in heterogeneous catalysis, Carbon 36 (1998) 159–175, https://doi.org/10.1016/S0008-6223(97)00173-5.
[17] M.O. Guerrero-Perez, J.M. Rosas, R. Lopez-Medina, M.A. Bañares, J. Rodriguez-Mirasol, T. Cordero, Lignocellulosic-derived catalysts for the selective oxidation of

propane, Catal. Commun. 12 (2011) 989–992, https://doi.org/10.1016/j.catcom.2011.03.010.
[18] Y.J. Lee, L. Radovic, Oxidation inhibition effects of phosphorus and boron in different carbon fabrics, Carbon 41 (2003) 1987–1997. ⟨https://www.sciencedirect.com/science/article/pii/S0008622303001994⟩.
[19] M.O. Guerrero-Perez, Research progress on the applications of electrospun nanofibers in catalysis, Catalysts 12 (2022) 9, https://doi.org/10.3390/catal12010009.
[20] S. Thenmozhi, N. Dharmaraj, K. Kadirvelu, H.Y. Kim, Electrospun nanofibers: New generation materials for advanced applications, Mat. Sci. Eng. B: Solid-State Mat. Adv. Tech. 217 (2017) 36–48, https://doi.org/10.1016/j.mseb.2017.01.001.
[21] R. Berenguer, J. Fornells, F.J. García-Mateos, M.O. Guerrero-Pérez, J. Rodríguez-Mirasol, T. Cordero, Novel synthesis method of porous VPO catalysts with fibrous structure by electrospinning, Catal. Today 277 (2016) 266–273, https://doi.org/10.1016/j.cattod.2016.03.002.
[22] X.K. Li, W.-J. Ji, J. Zhao, Z.B. Zhang, C.T. Au, n-Butane oxidation over VPO catalysts supported on SBA-15, J. Catal. 238 (2006) 232–241, https://doi.org/10.1016/j.jcat.2005.12.012.
[23] F.B. Abdelouahab, R. Olier, N. Guilhaume, F. Lefebvre, J.C. Volta, A study by in situ laser Raman spectroscopy of VPO catalysts for n-butane oxidation to maleic anhydride, J. Catal. 134 (1992) 151–167, https://doi.org/10.1016/0021-9517(92)90218-7.
[24] E.W. Arnold, S. Sundaresan, Effect of water vapor on the activity and selectivity characteristics of a vanadium phosphate catalyst towards butane oxidation, Appl. Catal. 41 (1988) 225–239, https://doi.org/10.1016/S0166-9834(00)80394-2.
[25] R.M. Contractor, H.S. Horowith, G.M. Sisler, E. Bordes, The effects of steam on n-butane oxidation over VPO as studied in a riser reactor, Catal. Today 37 (1997) 51–57, https://doi.org/10.1016/S0920-5861(96)00257-X.